Study of Induction Chemotherapy Efficacy in Oral Squamous Cell Carcinoma Using Pseudotargeted Metabolomics

ARTICLE *in* JOURNAL OF PROTEOME RESEARCH · FEBRUARY 2014

Impact Factor: 4.25 · DOI: 10.1021/pr4011298 · Source: PubMed

Journal of proteome research

Article

pubs.acs.org/jpr

Study of Induction Chemotherapy Efficacy in Oral Squamous Cell Carcinoma Using Pseudotargeted Metabolomics

Guozhu Ye,[†,§] Ying Liu,[‡,§] Peiyuan Yin,[†] Zhongda Zeng,[†] Qiang Huang,[†] Hongwei Kong,[†] Xin Lu,[†] Laiping Zhong,*[,‡] Zhiyuan Zhang,[‡] and Guowang Xu*[,†]

[†]Key Laboratory of Separation Science for Analytical Chemistry, Dalian Institute of Chemical Physics, Chinese Academy of Sciences, 457 Zhongshan Road, Dalian 116023, China

[‡]Department of Oral & Maxillofacial-Head & Neck Oncology, Ninth People's Hospital, Shanghai Jiao Tong University School of Medicine, No. 639 Zhizaoju Road, Shanghai 200011, China

Supporting Information

ABSTRACT: The effect of induction chemotherapy on oral cancer is controversial owing to inconsistent results. However, the efficacy of induction chemotherapy is closely related to locoregional recurrence, distant metastasis, and overall survival after the treatment. A pseudotargeted metabolomics revealed that metabolites involved in glycolysis and amino acid metabolism were inversely regulated in patients with different chemotherapy responses, and most fatty acids, steroids, and antioxidant substances were up-regulated in all patients after the treatment. Among the metabolites, lactic acid, glucose, glutamic acid, aspartic acid, leucine, and glycerol were remarkably associated with induction chemotherapy efficacy. Subsequently, lactic acid, glutamic acid, and aspartic acid were defined as potential biomarkers of the suitability and efficacy of induction chemotherapy. Our results show that 100.0 and 84.37% of patients with different chemotherapy efficacy were correctly identified in the training and test sets, respectively. Moreover, patient suitability for treatment was correctly predicted for 100.0, 81.25, and 100.0% of patients in the training, test, and external validation sets, respectively. In conclusion, metabolites related to glycolysis, redox homeostasis, and anabolic progress were indicative of induction chemotherapy efficacy both pre- and post-chemotherapy and beneficial for outcome evaluation and prediction. These results illustrate the potentials of metabolomics in personalized induction chemotherapy.

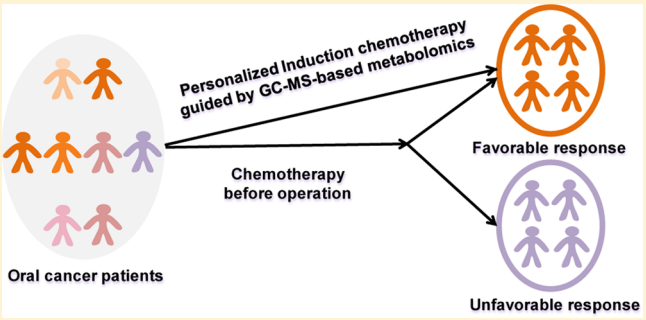

KEYWORDS: *pseudotargeted metabolomics, oral squamous cell carcinoma, potential biomarkers, induction chemotherapy, metabolomics, personalized medicine*

INTRODUCTION

Oral squamous cell carcinoma (OSCC), the most prevalent oral tumor, is associated with high mortality and a low overall 5 year survival rate (50−60%) despite progress in clinical examination, surgery, postoperative chemotherapy, and radiotherapy.[1,2] Poor prognosis occurs in patients with aggressive solid tumors, chemotherapy-resistant recurrence, or metastases after treatment.[3,4] However, heterogeneous results prevent firm conclusions from being drawn with regard to chemotherapy efficacy.[5] Induction chemotherapy, which uses chemotherapeutic drugs as initial treatment prior to radiotherapy or surgery of cancer, has attracted great attention. Nevertheless, a favorable pathologic response to TPF (docetaxel, cisplation, and fluorouracil) induction chemotherapy (viable tumor cells ≤10%), which is closely associated with increased overall survival and decreased locoregional recurrences and distant metastases, was observed in only 27.7% of OSCC patients.[4] Accordingly, better insight into the molecular mechanisms related to OSCC physiopathology, biomarker discovery, and treatment response is essential for the improvements of prognosis, therapeutic efficacy, and individualized treatment.

The application of metabolomics in cancer pathophysiology, biomarker discovery, and treatment response has attracted increasing attention.[6−12] Lysophosphatidylcholine 22:5, lysophosphoethanolamine 16:0, and taurocholic acid have been defined as potential biomarkers for the staging of diethylnitrosamine-induced hepatocarcinogenesis and further validated by the successful identification of patients with small liver cancer.[6] Additionally, fatty acids released by mesenchymal stem cells during chemotherapy induction with platinum analogs have been associated with chemotherapy resistance.[9] Moreover, the glutathione metabolism pathway, the pentose phosphate pathway, glycolysis, and gluconeogenesis were found to be key mediators of the response to treatments using vehicle or BIBW 2992.[10]

Received: November 16, 2013
Published: February 19, 2014

Table 1. Demographic Information of the Subjects

subject characteristics		S		NS		
		no.	percentage (%)	no.	percentage (%)	p^a
age (years)	median (range)	52 (35−74)		53 (45−71)		
sex	male	7	31.8	15	68.2	0.652
	female	4	40.0	6	60.0	
clinical stage	III	6	28.6	15	71.4	0.340
	IV	5	45.5	6	54.5	
T[b]	T2	3	30.0	7	70.0	0.464
	T3	6	31.6	13	68.4	
	T4	2	66.7	1	33.3	
N[c]	N0	5	33.3	10	66.7	0.696
	N1	4	44.4	5	55.6	
	N2	2	25.0	6	75.0	
site[d]	tongue	4	23.5	13	76.5	0.169
	others	7	46.7	8	53.3	
remission rate[e]	SD	0	0.0	1	100.0	0.036
	PR	8	28.6	20	71.4	
	CR	3	100.0	0	0.0	
smoking status[f]	smoker	4	33.3	8	66.7	0.923
	nonsmoker	7	35.0	13	65.0	
alcohol use[g]	drinker	2	20.0	8	80.0	0.248
	nondrinker	9	40.9	13	59.1	

[a]p value was obtained from chi-square test. [b]T indicates the size of primary tumor. [c]N indicates the status of regional lymph nodes. [d]Others: including subgingival, supragingival, genal, gnathic, mouth floor, and retromolar sites. [e]SD: stable disease; PR: partial response; CR: complete response. [f]Smoker: smoking more than one package of cigarettes (20 cigarettes) daily per year; nonsmoker: without smoking history. [g]Drinker: at least 10 year history of one drink per day; nondrinker: without drinking history.

The pseudotargeted metabolomics approach is a novel nontargeted metabolomics analytical method; it acquires the metabolome data by using the targeted method (i.e., gas chromatography−mass spectrometry (GC−MS)−selective ion monitoring (SIM), GC−MS MRM (multiple reaction monitoring), or high-performance liquid chromatography (HPLC)−MS MRM) based on the characteristic ion information obtained from the nontargeted metabolomics data without the aid of standard references. It integrates the advantages of targeted and untargeted methods (wider linearity, higher sensitivity, increased data quality compared with the full scan method, etc.).[13,14] In the current study, samples from OSCC patients with different pathologic responses to TPF induction chemotherapy were subdivided for further investigations.[4] A GC−MS-based pseudotargeted metabolomics approach was developed to obtain the metabolic signatures of OSCC patients in response to TPF induction chemotherapy. The findings were also used to advance the discovery of biomarkers of chemotherapy efficacy and prediction of suitability for induction chemotherapy.

MATERIALS AND METHODS

Materials and Chemicals

HPLC-grade methanol and dichloromethane were purchased from Merck (Germany) and Sigma-Aldrich China (Shanghai, China), respectively. Tridecanoic acid (≥98%), pyridine (CHROMASOLV plus, for HPLC, ≥ 99.9%), methoxyamine hydrochloride (98%), and MSTFA (*N*-methyl-*N*-(trimethylsilyl)-trifluoroacetamide, for GC derivatization, ≥98.5%) were all obtained from Sigma-Aldrich. Reference standards for compound identification and validation were the products of Alfa Aesar China (Tianjin, China), Sigma-Aldrich, or J&K Scientific (Beijing, China).

Subject Enrollments and the Treatment

Signed consent was obtained from all enrolled patients, and the study was performed in accordance with the Helsinki declaration under the authority of the Ethics Committee of Shanghai Ninth People's Hospital, Shanghai Jiao Tong University School of Medicine.

Patients with locally advanced OSCC (oral cavity origination) were histopathologically verified. Details of patient enrollment could be referred to the criteria.[4] Chiefly, all patients were at clinical stage III or IVA, according to the TNM staging system (UICC 2002), and the lesions were evaluated as resectable from the point of surgeons. Other main criteria included ALT (alanine aminotransferase) and AST (aspartate aminotransferase) below 2.5 times the upper limit of the normal level, hemoglobin above 8 g/L, Karnofsky performance status above 60%, bilirubin and serum creatinine below 1.5 times the upper limit of the normal level, WBC (white blood cell) count above 3000/μL, and platelet count above 80 000/μL. Besides, it was confirmed that there were no distant metastasis, previous chemotherapy/radiotherapy, other types of malignancies, or creatinine clearance below 30 mL/min in recruited patients. Demographic information of the patients is provided in Table 1 as well.

The detailed protocol of TPF induction chemotherapy was referable in the treatment.[4] In brief, intravenous docetaxel (75 mg/m^2 on first day), cisplatin (75 mg/m^2, on first day), and fluorouracil (750 mg/m^2, in a continuous manner from first to fifth days) were included in each cycle of induction chemotherapy treatment. The treatment was conducted two cycles during a 3 week period except when the disease progressed or an unacceptable toxicity emerged. Administration of antiemetics, prophylactic antibiotics, dexamethasone, and hydration/diuretics was initiated on the fifth day of each cycle for 3 days. Moreover, decreases in chemotherapy dose were permitted

dx.doi.org/10.1021/pr4011298 | J. Proteome Res. 2014, 13, 1994−2004

under the condition of grade 3 to 4 toxicities after first cycle treatment.

Related serum samples from enrolled patients were all collected under fasting conditions. The prechemotherapy samples were collected the next morning after the patients were hospitalized, and postchemotherapy samples were sampled 2 to 3 weeks after induction chemotherapy. All of the collected samples were stored at −80 °C. Evaluation of induction chemotherapy efficacy was based on clinical manifestation and image investigations of the patients, which were successively carried out before induction chemotherapy and 2 weeks after second cycle of the treatment. Detailed information on the assessment of clinical tumor response could be referred to the chemotherapy in OSCC patients as well.[4,15]

Sample Classifications according to the Clinical Response

On the basis of the clinical response, the effects of induction chemotherapy were defined as significant if <10% of tumor cells remained. Subsequently, the patients were classified into the following categories: SPre (prechemotherapy patients with significant chemotherapy efficacy), SPost (postchemotherapy patients with significant chemotherapy efficacy), NSPre (prechemotherapy patients with nonsignificant chemotherapy efficacy), NSPost (postchemotherapy patients with nonsignificant chemotherapy efficacy), S (patients with significant chemotherapy efficacy), and NS (patients with nonsignificant chemotherapy efficacy). In total, 11 pairs of SPre and SPost and 21 pairs of NSPre and NSPost samples were examined.

To further confirm the prechemotherapy predictability of treatment outcomes, an additional batch of samples (comprising 4 SPre and 14 NSPre samples) was collected from Shanghai Ninth People's Hospital, and the criteria for pathological confirmation and sample collection were in line with those previously described.

Sample Preparation

After thawing at room temperature and then being vortex-mixed for 10 s, 100 μL of serum from each sample was pipetted into Eppendorf tube; meanwhile, equal aliquots of all analytical samples were drawn and mixed well for 5 min for the preparation of QC (quality control) samples. QC samples were treated in the same way as other analytical samples. One QC sample was inserted every 10 analytical samples.

400 μL of ice-cold methanol (including 40 μg/mL tridecanoic acid as the internal standard) was added to 100 μL of serum sample and vortex-mixed thoroughly for 30 s to precipitate proteins and extract the metabolites as completely as possible. After centrifugation at 15 000*g*, 4 °C for 15 min, 360 μL supernatant was transferred for vacuum drying in CentriVap Centrifugal Vacuum Concentrators (Labconco, MO). Thereafter, 100 μL of methoxyamine pyridine solution (20 mg/mL) was added to the dried sample, vortex-mixed for 30 s, then ultrasound-treated for 10 min to dissolve as many metabolites as possible. Then, a 2 h oximation reaction was conducted in 40 °C water bath, followed by silylation reaction with 80 μL of MSTFA for 1 h in 40 °C water bath as well. After derivatization, the solution was centrifuged again under the conditions of 15 000*g*, 4 °C for 15 min for the precipitation of metabolites undissolved in the solution, avoiding unrepeatable results. Ultimately, the supernatant of the derivatized solution was diverted to a 2 mL glass vial with an inserted liner and analyzed by GC−MS afterward.

Establishment of SIM Scan Table for Pseudotargeted Metabolomics Method

Full Scan Acquisition of the QC Sample. Serum metabolic profiling of the QC sample was analyzed using the GCMS-QP 2010 analytical system with a quadrupole mass analyzer and AOC-20i autosampler (Shimadzu, Kyoto, Japan). Chromatographic separations of derivatized metabolites were accomplished on a DB-5 MS capillary column (30 m × 250 μm × 0.25 μm, J&W Scientific, Folsom, CA). The constant flow rate of carrier gas (helium) via the column was operated at 1.19 mL/min in the event that the linear velocity was set at 40.0 cm/s. The oven temperature was initially set to 70 °C, held for 3 min, and then increased to 300 °C at a rate of 5 °C/min, and finally kept for 5 min. Temperatures of inlet, interface, and ion source were manipulated at 300, 280, and 230 °C, respectively. Detector voltage was set at 1.17 kV, and EI (electron impact, 70 eV) was applied as the ionization mode. Mass signal acquisition (33−600, m/z) was performed by workstation GCMS solution 2.7 (Shimadzu, Kyoto, Japan) after 6.0 min of solvent delay, and the event time was set at 0.5 s.

Deconvolution and Identification of Full Scan Data from the QC Sample. Raw MS data acquired from GCMS solution were first converted to netCDF format, which could be imported into AMDIS 2.62 (NIST, USA) and ChromaTOF 4.43 (LECO Corporation, USA) for mass spectra detection, deconvolution, and identification. The peak width and S/N (signal-to-noise) were set to 4 s and 50, respectively, in the process of mass spectra by ChromaTOF sofware. Metabolite identification was conducted on the basis of our previous work.[12] In brief, the metabolites were identified through a mass spectra search against those of standards in commercial libraries (NIST 11, Wiley, and Fiehn) and the available reference standards. Additionally, the retention times and retention indexes of the reference standards were employed for determining elution orders of the metabolites, which was beneficial to distinguishing the metabolites with similar mass spectra, apart from auxiliary structure validation.

Establishment of SIM Scan Table for Pseudotargeted Metabolomics Method Targeted Metabolic Profiling. Establishment of SIM scan table was carried out in the light of the pseudotargeted method with a few modifications.[13] The process of establishment of SIM scan table was principally composed of mass spectrum detection and full-scan data deconvolution in the QC sample, obtaining the time of starting, vertex and terminal points of the peaks, feature ion selection, and grouping.[13] The workflow for establishment of SIM scan table is provided in Figure S1 (Supporting Information). Parameters for mass spectra detection and deconvolution using AMDIS were set in line with the default values. Peaks with abundance <1000 or S/N <20 were removed. Moreover, among the successively adjacent peaks (interval of scan points <4), only the most intensive peak was retained in the peak table. To improve the MS responses of lower content metabolites, the injection volume was increased and the split ratio was reduced. Under these conditions, more metabolites were identified and then replenished in the SIM table (Figure S1, Supporting Information). With regard to the coeluted isomers with almost identical mass spectra, feature ions were required to be manually assigned by referring to the relative response of target peaks to the interference peaks, and the characteristic ions were provided by ChromaTOF software.

dx.doi.org/10.1021/pr4011298 | J. Proteome Res. 2014, 13, 1994−2004

Data Acquisitions of Metabolic Profiling in Pseudotargeted Mode

For the collection of metabolic profiling data in pseudotargeted mode, all samples were analyzed using the integrated SIM scan table under the condition that the injection volume and split ratio were set to 1 μL and 10:1, respectively (Figure S1, Supporting Information). The event time was adjusted to 0.2 s based on the recommendatory setting. Other GC−MS parameters were the same as those previously described in full scan. Dichloromethane solution was injected three times for the elution of impurities primarily from inlet, liner, and the column, followed by 10 injections of the same QC sample to balance the analytical system. One QC sample was analyzed every 10 analytical samples to evaluate the reproducibility and repeatability of the analytical sequence.

After running all samples, the retention times of *n*-alkanes, necessary for obtaining Kovat's retention index of the serum metabolites, were acquired by the analysis of a light diesel sample in full-scan mode.

In the validation of discovered metabolites for discriminating SPre from NSPre patients, targeted analysis was put to use, where lactic acid, leucine, aspartic acid, glutamic acid, glycerol, glucose, and tridecanoic acid were targeted in another new SIM scan table. Detector voltage was adjusted to 1.27 kV according to the tuning voltage, and other parameters of instrumental analysis and sample pretreatment were not changed.

Data Processing

Quantitative table of the unique ions for detected metabolites was created according to the final SIM scan table and imported into GCMS solution for batch integration of the analytical samples. Afterward, ion peak area of the metabolite was normalized to the internal standard and multiplied by 1×10^6, then utilized for following data processing.

Principal component analysis (PCA) was first utilized to visualize the distribution of QC and other samples for the reproducibility evaluation of serum metabolic profiling employing SIMCA-P 11.0 (Umetrics, Sweden). Nonparametric test using PASW Statistics 18 (IBM, Chicago, IL) was introduced to the pairwise comparisons of the induction chemotherapy samples to discover the pathophysiological alterations in response to induction chemotherapy and the metabolic signatures concerned with chemotherapy effects. The differential metabolites were uncovered based on p value of bilateral asymptotic significance (Mann−Whitney U test, $p < 0.05$). Heat map employing MeV 4.7.4 was carried out to project the metabolic regulations of the differential metabolites due to induction chemotherapy treatment and the metabolic discrepancies among patients having different chemotherapy responses.[16] PLS-DA (partial least-squares discriminant analysis), PCA, pathway analysis, and correlation analysis were performed by means of MetaboAnalyst 2.0, and p cutoff value was set to 0.05 in the pathway analysis and correlation analysis.[17] PLS-DA and PCA were implemented to present the influence of induction chemotherapy. Pathway analysis was utilized to uncover the pathways significantly correlated with induction chemotherapy efficacy. In addition, correlation analysis was executed to discover the metabolites remarkably related to chemotherapy effects under different conditions. Chi-square test and rank sum test were both conducted via PASW Statistics 18. Demographic differences related to chemotherapy effects according to various clinical factors were revealed by chi-square test). The metabolic differences of the differential metabolites associated with chemotherapy effects in response to clinical factors were uncovered by rank sum test.

Variable importance in projection (VIP) method and random forest (RF) method were developed in Matlab (MathWorks, Natick, MA) for variable selection and constructing classification models, respectively, to obtain the potential metabolites for assessments of induction chemotherapy efficacy and patient suitability for induction chemotherapy.[18−20] Furthermore, 1000 times of Monte Carlo cross validation (MCCV), which had abundant mathematical foundations to evaluate the generalization ability of fitting models, was applied to generate reliable results through random division of samples for the determination of training and test sets.[21−23] Then, the error rates for discrimination and prediction of each sample were individually counted among the entire MCCV results and ultimately averaged to characterize the performance of the corresponding sample. The results of ROC (receiver operating characteristic) curves and final error rates of training, test, and validation sets were on the basis of these outcomes, which should guarantee the reliability of potential biomarkers for wide and large independent validation. The scheme of potential biomarker discovery and the performance evaluation can be viewed in Figures S2 and S3 (Supporting Information).

RESULTS

Analytical Performance of Serum Metabolic Profiling in Pseudotargeted Mode

After MS data processing, 258 peaks were defined in the final SIM scan table. On the basis of a previously described method of metabolite identification,[12] 142 metabolites were identified (Table S1, Supporting Information). Compared with the full scan, the S/N was improved in 88.0% of the metabolites included in the SIM scan, especially low-abundant metabolites. In addition, overlapping peaks were more effectively deconvoluted in the SIM scan than in the full scan (Figure S4 and S5, Supporting Information). Among all samples, seven QC samples were tightly clustered in the PCA plot and displayed good linear relationships, the pairwise Pearson correlation coefficients ranged from 0.998 to 1.000; furthermore, the relative standard deviation of the contents in 67.7, 77.0, and 88.3% of the detected metabolites in seven QC samples was lower than 15, 20, and 30%, respectively, throughout the experiment (Table S2 and Figure S6, Supporting Information). It is recommended that QC samples should be located closely;[24] 60% of the metabolites should lie within 15% of their mean, with a more relaxed criterion (20%) for the metabolites near their limit of quantification.[25,26] Altogether, these data suggest that the serum metabolic profiles acquired in pseudotargeted mode were stable and reproducible.

Discovery of Differential Metabolites

Using the metabolite identification method,[12] 49 metabolites with $p < 0.05$ were identified from five pairwise sample comparisons (Table S3, Supporting Information). Among the identified metabolites, 43 corresponded to metabolites in the MetaboAnalyst libraries of pathway analysis and 37 were confirmed using reference standards.

Global Metabolic Alterations in Response to Induction Chemotherapy

In the PLS-DA model, the postchemotherapy and prechemotherapy samples were apparently different, and the classification

dx.doi.org/10.1021/pr4011298 | J. Proteome Res. 2014, 13, 1994−2004

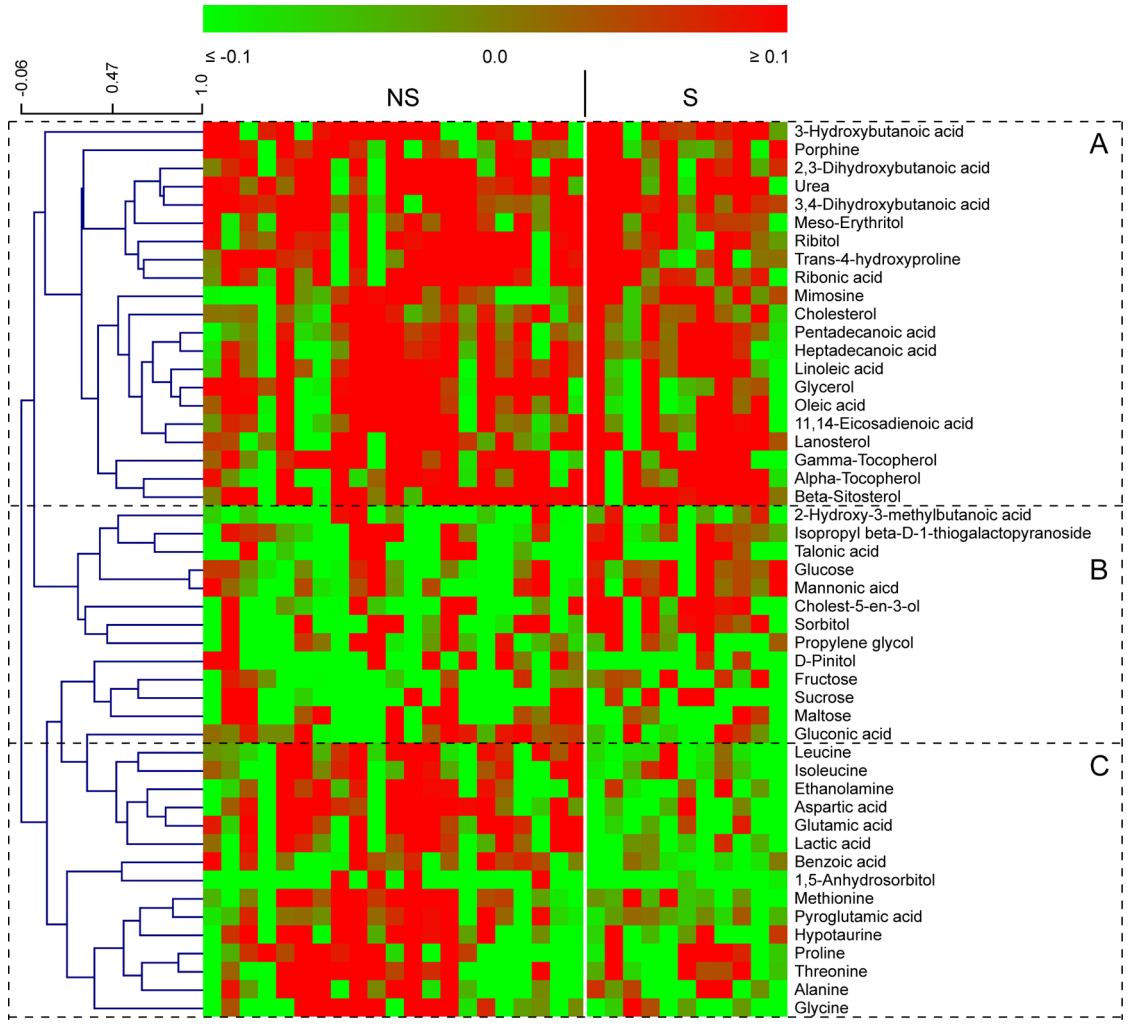

Figure 1. Heat map demonstration of the changes in the differential metabolites. Data were from the differential metabolites (Table S2, Supporting Information). The ratio of postchemotherapy level to prechemotherapy level (from the same patient) for each metabolite was first computed, and then alterations of the differential metabolites were expressed as lg (ratio), which was applied for the heat map analysis. Most metabolites in panel A were up-regulated after chemotherapy, whereas most metabolites in panel B were down-regulated after chemotherapy in both S and NS patients. In panel C, most metabolites in S were inversely regulated between S and NS patients.

performance was stable and reliable (Figure S7, Supporting Information). The substantial separation of the postchemotherapy and prechemotherapy samples indicates the impact of induction chemotherapy on the metabolic profile, and the major metabolic effects of chemotherapy were thus visualized in a plot (Figure 1). According to metabolite clustering, the metabolic changes in response to induction chemotherapy were visually classified into three panels. Following chemotherapy, most of the metabolites in panel A (primarily fatty acids, steroids, and antioxidant substances) were up-regulated, whereas most of the metabolites in panel B (principally involved in carbohydrate metabolism) were down-regulated in OSCC patients. Moreover, a large proportion of the metabolites in panel C (primarily amino acids in addition to lactic acid and ethanolamine) and glycerol (panel A) were up-regulated in NS patients, whereas these metabolites were down-regulated in S patients after induction chemotherapy. In addition, levels of glucose and mannonic acid decreased in NS patients but increased in S patients receiving chemotherapy (panel B). Inverse trends in the metabolic changes due to induction chemotherapy between S and NS patients (primarily in panel C) potentially indicate the metabolic differences among patients with different chemotherapy efficacy.

Metabolic Characteristics Related to Induction Chemotherapy Efficacy

Pathway analysis revealed a marked difference in amino acid and carbohydrate metabolism between NS and S patients responding to chemotherapy (Table S4, Supporting Information). The major metabolites involved in these metabolic pathways were aspartate, glutamate, lactic acid, glucose, glycine, leucine, isoleucine, pyroglutamic acid, methionine, and glycerol. These metabolites exhibited differential trends in S and NS patients after induction chemotherapy, and their regulations were distinct and strongly correlated in response to induction chemotherapy (Figure S8, Supporting Information).

In the correlation analysis, metabolic perturbations of aspartic acid, glutamic acid, glycerol, lactic acid, leucine, and glucose were markedly associated with the effects of induction chemotherapy, and all of the metabolites were inversely regulated in S and NS patients in response to induction chemotherapy (Figures 2A and 3). In particular, levels of lactic acid, glutamic acid, aspartic acid, and leucine were all

dx.doi.org/10.1021/pr4011298 | J. Proteome Res. 2014, 13, 1994−2004

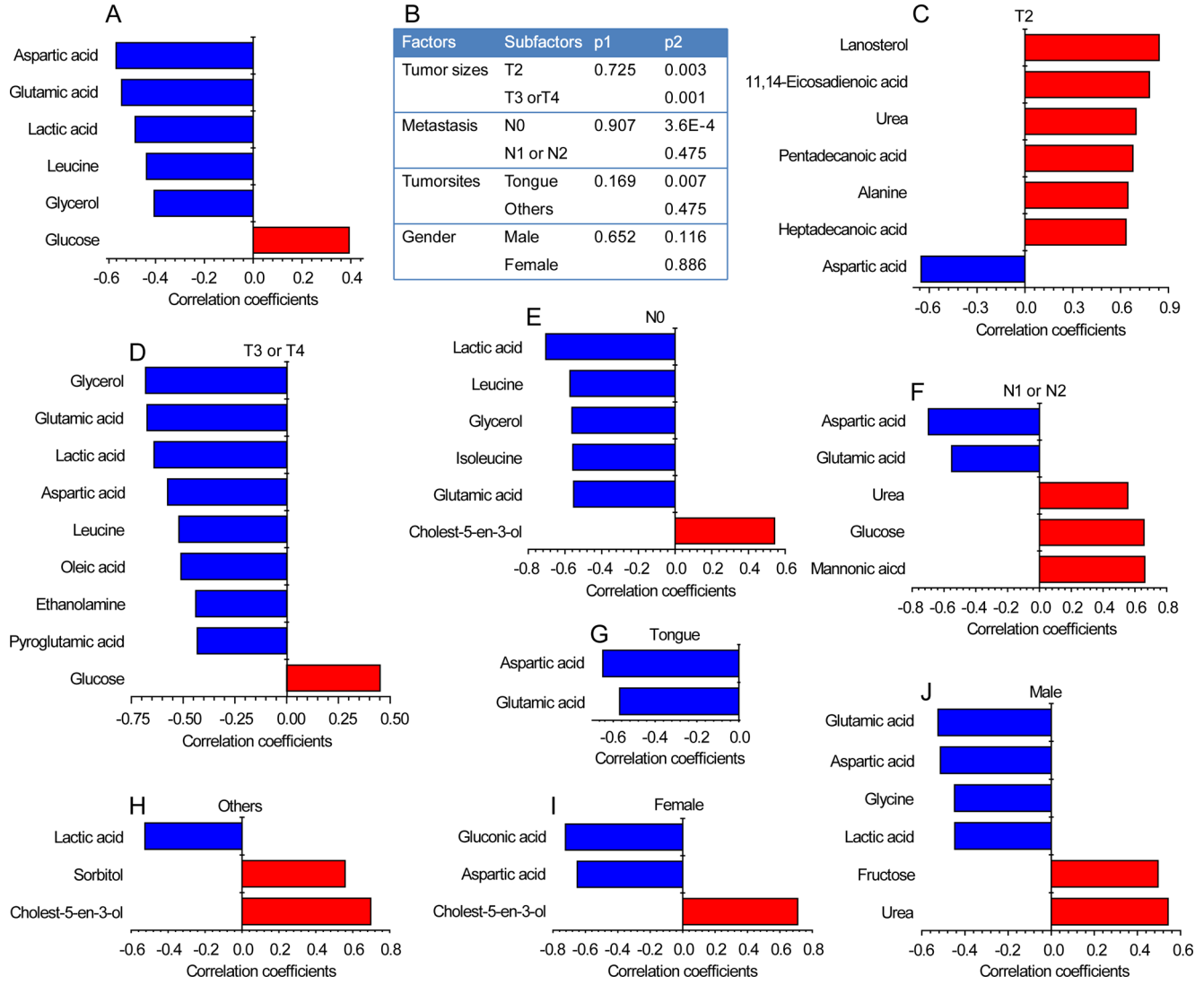

Factors	Subfactors	p1	p2
Tumor sizes	T2	0.725	0.003
	T3 orT4		0.001
Metastasis	N0	0.907	3.6E-4
	N1 or N2		0.475
Tumorsites	Tongue	0.169	0.007
	Others		0.475
Gender	Male	0.652	0.116
	Female		0.886

Figure 2. Key metabolites and clinical factors associated with induction chemotherapy efficacy. Data were from the differential metabolites (Table S2, Supporting Information). The ratio of the postchemotherapy level to the matched prechemotherapy level was used for comparison of NS patients and S patients with specific clinical backgrounds. Pattern correlation analysis was performed in panels A and C−J. Alterations in key metabolites related to chemotherapy efficacy specific for clinical factors are provided in Figure S10−S17 (Supporting Information). (A) Metabolites related to chemotherapeutic efficacy independent of clinical characteristics. (B) Influences of clinical factors on induction chemotherapy efficacy. $p1$ was obtained from chi-square test for the differences in chemotherapy efficacy based on demographic data; $p2$ was obtained from rank sum tests for differences in chemotherapy efficacy based on differential metabolite information (Table S2, Supporting Information). (C−F) Metabolites related to differences in chemotherapy efficacy among T2, T3, or T4 and N0, N1, or N2 stages, respectively. (G,H) Metabolites related to differences in chemotherapy efficacy in tongue tumors and nontongue tumors, respectively. (I,J) Metabolites related to differences in chemotherapy efficacy in female and male patients, respectively.

significantly decreased in S patients (SPost vs SPre, p = 0.008, 0.039, 0.020, and 0.028, respectively) and increased in NS patients. After induction chemotherapy, levels of glycerol were prominently increased in NS patients (NSPre vs NSPost, p = 0.009) and decreased in S patients. In contrast, levels of glucose were increased in S patients but decreased in NS patients following chemotherapy. Furthermore, it is important to note that basal levels of lactic acid, glutamic acid, aspartic acid and leucine were significantly higher in S patients than in NS patients prior to induction chemotherapy (SPre vs NSPre, p = 0.016, 0.020, 0.023, and 0.015, respectively). In addition, glucose concentrations were significantly decreased in S patients relative to NS patients prior to induction chemotherapy (SPre vs NSPre, p = 0.005).

Other metabolites associated with induction chemotherapy efficacy are summarized in Figures S9 and S10 (Supporting Information). Levels of isoleucine, glycine, pyroglutamic acid, methionine, and hypotaurine were increased in S patients (SPost vs SPre) and decreased in NS patients (NSPost vs NSPre) in response to induction chemotherapy. In addition, the concentration of isoleucine was significantly different between prechemotherapy S and NS patients (SPre vs NSPre, p = 0.023). Moreover, levels of pyroglutamic acid, methionine, hypotaurine, threonine, proline, and alanine following chemotherapy were significantly lower in S patients than in NS patients (SPost vs NSPost, p = 0.045, 0.045, 0.016, 0.009, 0.0495 and 0.0495, respectively).

With regard to fatty acid metabolism, levels of linoleic acid, oleic acid, and 11,14-eicosadienoic acid were significantly

dx.doi.org/10.1021/pr4011298 | J. Proteome Res. 2014, 13, 1994−2004

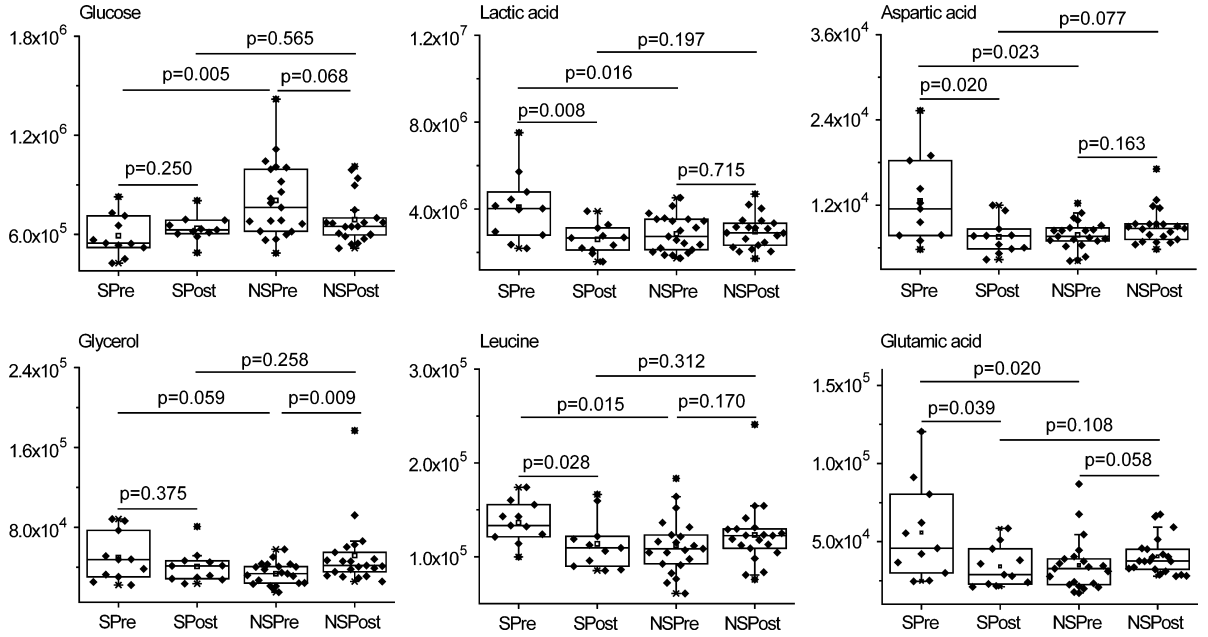

Figure 3. Metabolic alterations of the key metabolites associated with chemotherapy efficacy independent of clinical factors. The key metabolites were discovered by correlation analysis ($p < 0.05$).

increased in NS patients (NSPost vs NSPre, $p = 0.028$, 0.02 and 0.007, separately), whereas no significant changes in these metabolites were observed in S patients (SPost vs SPre, $p = 0.491$, 0.622, and 0.178, respectively). In addition, levels of 3-hydroxybutanoic acid increased in NS patients after chemotherapy (NSPost vs NSPre, $p = 0.046$), whereas the response in S patients was not significant (SPost vs SPre, $p = 0.279$). Furthermore, strong relationships among metabolites associated with fatty acid metabolism in response to the chemotherapy treatment were evident (Figure S8, Supporting Information).

Moreover, levels of cholesterol, lanosterol, beta-sitosterol, alpha-tocopherol, and gamma-tocopherol were increased in both S and NS patients following chemotherapy. Levels of ethanolamine were reduced in S patients but increased in NS patients in response to chemotherapy treatment; meanwhile, levels of ethanolamine were markedly higher in NS patients than in S patients after chemotherapy (NSPost vs SPost, $p = 0.023$).

Influence of Induction Chemotherapy on Key Metabolites in Patients with Different Clinical Parameters

The impacts of clinical parameters (tumor size, metastasis status, sex, and tumor site) on induction chemotherapy efficacy were further studied to identify relevant factors affecting key metabolites. Although there were no remarkable differences with regard to demographic data, notable metabolic differences in response to chemotherapy were observed in patients with different clinical backgrounds (Figure 2B). Metabolic modulation of lactic acid, aspartic acid, glutamic acid, glycerol, glucose, and leucine was associated with chemotherapy efficacy in patients with T3 or T4 stage, and metabolic changes in lactic acid, leucine, glutamic acid, and glycerol were significantly correlated with the chemotherapy efficacy in N0 stage. In addition, alterations in aspartic acid and glutamic acid levels were markedly associated with the effects of chemotherapy in N1 and N2 stage, tongue tumors, and male patients. Moreover, lactic acid content was significantly associated with chemotherapy efficacy in male patients and nontongue tumors (Figure 2). Compared with other clinical characteristics, tumor size (T3 or T4) and metastasis status (N0) appear to be critically involved in the regulation of key metabolites associated with the efficacy of induction chemotherapy. Furthermore, the differences in the key metabolites occurred in S and NS patients were independent of clinical parameter, which indicates that these key metabolites are useful in predicting the treatment efficacy (Figure S11−S18, Supporting Information). Additionally, prechemotherapy differences between S and NS patients were distinct, and levels of most metabolites related to chemotherapy efficacy were considerably higher in S patients than in NS patients (S11−S18, Supporting Information).

Potential Biomarkers for Evaluating Induction Chemotherapy Efficacy

As previously described, the key metabolites identified by the correlation analysis are indicative of not only the metabolic alterations in response to induction chemotherapy but also chemotherapy efficacy (Figures 1 and 3). Therefore, we used these key metabolites to evaluate chemotherapy efficacy.

To assess chemotherapy responses, key metabolites associated with chemotherapy efficacy (Figure 3) were first introduced for variable selections using the VIP method in the data set (including training set and test set).[18,19] Then, lactic acid, glutamic acid, and aspartic acid were defined as candidate biomarkers for chemotherapy efficacy and further employed in the RF model for assessing the diagnostic performance of potential biomarkers.[20] Following the variable selection, samples were randomly divided into two cohorts at a 2:1 ratio of training set to test set using the MCCV method in each modeling process.[21−23] After each cycle of sample division by the MCCV method, the RF model was built using the training data set and further utilized to evaluate diagnostic performances of the potential biomarker combination in the training set and test set. The cycle was conducted 1000 times, which could effectively reduce the false discovery and false positive. The predictive results of each sample in the training set and test set

dx.doi.org/10.1021/pr4011298 | J. Proteome Res. 2014, 13, 1994−2004

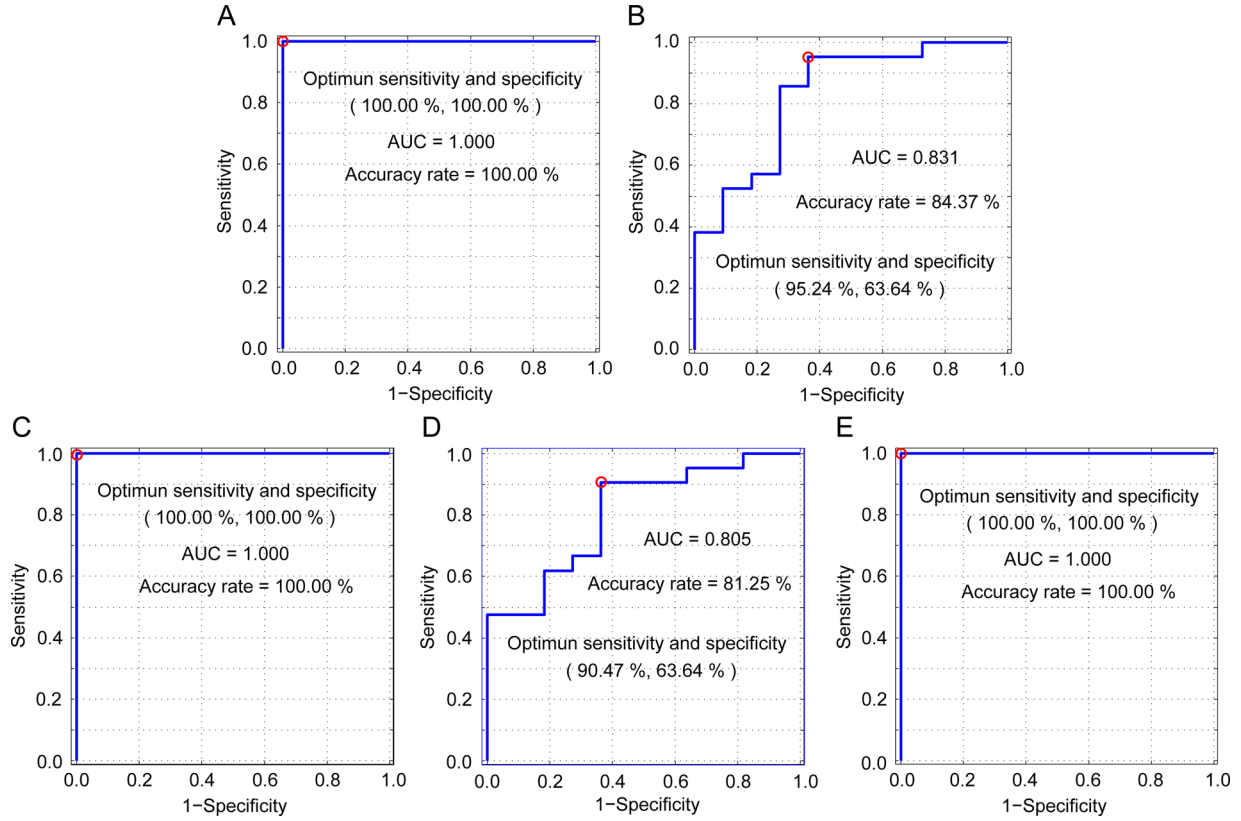

Figure 4. Evaluation and prediction of chemotherapy efficacy performed by a random forest algorithm. Both the accuracy rate and ROC plot were based on the discriminant results of individual samples, which were statistically processed by 1000 times of MCCV running. The sensitivity and specificity were optimized according to the summation. (A,B) Data utilized for evaluation of chemotherapy efficacy. Data were from the metabolites associated with induction chemotherapy efficacy (Figure 3), and the ratio of postchemotherapy levels to matched prechemotherapy levels was utilized for the analysis. (A) Discrimination of chemotherapy efficacy in the training set using the combination of lactic acid, glutamic acid, and aspartic acid. (B) Prediction of chemotherapy efficacy in the test set using the combination of lactic acid, glutamic acid, and aspartic acid. (C−E) Data utilized for the prediction of patient suitability for induction chemotherapy. Data were from the metabolites associated with induction chemotherapy efficacy in prechemotherapy samples (Figure 3). (C) Classification of chemotherapy efficacy prior to the treatment in the training set using the combination of lactic acid, glutamic acid, and aspartic acid. (D) Prediction of chemotherapy efficacy prior to the treatment in the test set using the combination of lactic acid, glutamic acid, and aspartic acid. (E) Validation of the prediction of patient suitability for induction chemotherapy employing new, independent samples. Lactic acid, glutamic acid, and aspartic acid were utilized for the validation.

in each discriminant process could be recorded and then averaged after 1000 times of cycles. The results showed that 100.0% of the patients in the training set (14 NS and 7 S) were correctly identified, and 84.37% of the patients in the test set (7 NS and 4 S) were accurately predicted. Moreover, the AUC (area under the curve) values were 1.000 and 0.831 in the training set and test set, respectively (Figure 4A,B). These data illustrate the outstanding performance of the combination of lactic acid, glutamic acid, and aspartic acid for evaluating the response to chemotherapy.

Potential Biomarkers to Predict the Suitability of Induction Chemotherapy

Only 27.7% of OSCC patients receiving the TPF induction chemotherapy presented a favorable pathologic response.[4] Therefore, the ability to predict patient suitability for TPF induction chemotherapy is critical and would prevent OSCC patients from ineffective treatments. It is important to note that patients with different responses to chemotherapy could be clearly distinguished prior to administration of chemotherapy (Figure S19, Supporting Information). In addition, the metabolites significantly related to chemotherapy efficacy showed prechemotherapy differences between S and NS patients (Figure 3), and high-performance prediction of induction chemotherapy efficacy was readily achieved, as the AUC value for each metabolite was higher than 0.7 (Figure S20, Supporting Information).

The key metabolites were also imported for variable screening by the VIP method in the data set (including the training set and test set) and used to classify the samples in the RF model. The process of variable selection and diagnostic evaluation of potential biomarkers in the training set and test set was previously described. Using the VIP method, lactic acid, glutamic acid, and aspartic acid were identified as potential biomarkers to predict patient suitability for induction chemotherapy treatment. Prechemotherapy metabolic differences between the 14 NS and 7 S patients in the training set were correctly distinguished by the three selected metabolites. Using these three potentially predictive biomarkers, 81.25% of the patients in the test set (7 NS and 4 S) were accurately classified, and AUC values of 1.000 and 0.805 were achieved in the training set and test set, respectively (Figure 4C,D). The classification results demonstrated satisfactory performance of lactic acid, glutamic acid, and aspartic acid as predictive biomarkers of patient suitability for treatment with induction chemotherapy.

dx.doi.org/10.1021/pr4011298 | J. Proteome Res. 2014, 13, 1994−2004

An additional batch of samples was collected, processed, and independently analyzed for external validation to further assess the applicability of lactic acid, glutamic acid, and aspartic acid as predictors of the response to induction chemotherapy. Lactic acid, glutamic acid, and aspartic acid were collectively employed in the RF model again to assess their predictability of patient suitability for induction chemotherapy. In this analysis, 4 SPre patients and 14 NSPre patients were all satisfactorily classified with a corresponding AUC value of 1.000 (Figure 4E), which effectively illustrated the potential clinical application of lactic acid, glutamic acid, and aspartic acid in predicting OSCC patient suitability for induction chemotherapy.

DISCUSSION

Metabolic Signatures Related to Induction Chemotherapy Efficacy

A remarkable decrease in lactic acid levels (SPost vs SPre, p = 0.008) and an increase in glucose levels in S patients indicated that glycolytic activity was largely decreased despite increased glucose availability in patients with significant chemotherapy efficacy following induction chemotherapy. Nevertheless, glucose levels decreased and lactic acid levels remained stable in NS patients receiving chemotherapy, which indicates that glycolytic activity remained elevated in patients with a poor response to chemotherapy, which was sustained by the notable increase in glycerol levels (NSPre vs NSPost, p = 0.009). The enhanced glycolytic activity, as observed in tumors, could provide a favorable environment for the survival and proliferation of residual tumor cells and counteract chemotherapeutic efficacy in patients with poor responses to chemotherapy.[27] Moreover, levels of alanine (a product of glycolysis and glutaminolysis and a precursor for pyruvate) were significantly increased in NS patients relative to S patients following chemotherapy (SPost vs NSPost, p = 0.0495). This finding suggests enhanced glycolytic activity or additional materials to meet the bioenergy demands of tumor cell proliferation and growth.

Levels of glycine, derived from glycolysis and also a precursor for purine nucleosides, were markedly decreased in S patients (SPre vs SPost, p = 0.039) but increased in NS patients following treatment, which is in agreement with the down-regulation of glycolytic activity in response to chemotherapy in patients with significant chemotherapy efficacy. Moreover, levels of threonine were markedly increased in NS patients compared with S patients after chemotherapy (NSPost vs SPost, p = 0.009). Threonine significantly contributes to the biosynthesis of glycine and acetyl-CoA, thus promoting one-carbon metabolism and replenishing tricarboxylic acid cycle.[28,29] Therefore, the remarkable increase in threonine and obviously high levels of glycine (SPost vs NSPost, p = 0.065) in NS patients relative to S patients illustrates not only a more vigorous methylation process but also greater oxidative stress in patients with poor efficacy following chemotherapy.

Metabolites including leucine, isoleucine, glutamic acid, aspartic acid, pyroglutamic acid, methionine, and hypotaurine were down-regulated in patients with significant chemotherapy efficacy and up-regulated in patients with poor responses. Glutamic acid, glycine, and pyroglutamic acid are amino acids critical for glutathione homeostasis, which plays a vital role in regulating in vivo redox states and removing reactive oxygen species (ROS).[30] Under hypoxic conditions, enhanced ROS production leads to oxidative stress, which cause the oxidization of glutathione and activates glutathione resynthesis.[10] Therefore, up-regulations of glutamic acid, glycine, pyroglutamic acid, methionine, and hypotaurine following chemotherapy are indicative of increased oxidative stress in patients with poor responses to chemotherapy. This phenomenon is further supported by the notable increase in gamma-tocopherol levels (NSPost vs NSPre, p = 0.039) in patients with poor outcomes. Moreover, a significant decrease in leucine (SPost vs SPre, p = 0.028) and isoleucine (SPost vs SPre, p = 0.061) levels in patients with effective responses to chemotherapy indicates reduced protein turnover or amino acid biosynthesis and fewer materials for biological energy as a result of chemotherapy.

Fatty acids were elevated in OSCC patients following chemotherapy. Oleic acid, linoleic acid, and 11,14-eicosadienoic acid were remarkably up-regulated in patients with poor efficacy (NSPre vs NSPost, p = 0.020, 0.028 and 0.007, respectively) but not in patients with significant chemotherapeutic efficacy (SPre vs SPost, p = 0.622, 0.491, and 0.178, separately). It is reported that polyunsaturated fatty acids induced by platinum are involved in the chemotherapy resistance of mesenchymal stem cells and that platinum-based chemotherapy combined with cyclooxygenase-1 or thromboxane inhibitors improves the chemotherapy efficacy.[9] In addition, metabolic differences of 3-hydroxybutanoic acid, ethanolamine, steroids, and other metabolites in patients with different chemotherapy efficacy were also observed.

Assessment of Induction Chemotherapy Efficacy and Prediction of Patient Suitability for Induction Chemotherapy

The metabolite combination of lactic acid, glutamic acid, and aspartic acid was able to successfully determine the chemotherapeutic efficacy and predict induction chemotherapy outcomes. As previously discussed, the potential biomarkers were principally involved in glycolysis and amino acid metabolism related to redox homeostasis, biomass renewals, and energy metabolism. According to the influences of relevant clinical factors on chemotherapy efficacy revealed by correlation analysis, it was clear that metabolic differences of lactic acid, glutamic acid, and aspartic acid among patients with different chemotherapy responses occurred in tumor sizes, metastasis status, gender, and tumor sites. Meanwhile, the metabolic differences of lactic acid, glutamic acid, and aspartic acid among patients with different chemotherapy efficacy were independent of investigated clinical parameters, which indicate that the combination of lactic acid, glutamic acid, and aspartic acid was applicable in relevant clinical backgrounds. Moreover, metabolites involved in glycolysis, gluconeogenesis, and amino acid metabolism related to redox homeostasis and de novo synthesis of biomass for new cells were suggestive of TPF treatment efficacy. As OSCC progresses from early stages to advanced stages, the metabolism shifts to anabolism, ROS detoxification, and corresponding energy adjustments (Figure S21, Supporting Information). Taken together, it is possible that efficacy of induction chemotherapy is related to the disease progression and that there is an ideal metabolic status, where the optimal chemotherapy efficacy could be achieved. The characteristics of this environment would include glycolysis, biomass renewals, and redox homeostasis, as revealed in the development of lung tumor and the chemotherapy responses.[10]

As revealed in the study, pharmacometabolomics, which is created by the application of metabolomics in the effects and variation of drug response,[31,32] is beneficial to discovering

dx.doi.org/10.1021/pr4011298 | J. Proteome Res. 2014, 13, 1994−2004

pathophysiologic variation in the response of induction chemotherapy, and the potential biomarkers could be utilized for the evaluation of chemotherapy outcomes and predicting the suitability for induction chemotherapy, thus contributing to the implementation of individualized induction chemotherapy in OSCC patients and illustrating the role of pharmacometabolomics.

CONCLUSIONS

A pseudotargeted metabolomic method was employed for delineating the metabolic regulations in response to induction chemotherapy and discovering potential biomarkers for evaluating chemotherapy outcomes and the suitability prediction of induction chemotherapy. Metabolic changes in carbohydrate metabolism, amino acid metabolism, fatty acid metabolism, steroid metabolism, and so on, were observed responding to induction chemotherapy. Furthermore, there were lower glycolytic activities and fewer materials for anabolic process and ROS detoxification in patients with favorable clinical response than those with poor outcomes after induction chemotherapy. Additionally, the metabolite combination of lactic acid, glutamic acid, and aspartic acid was useful not only for the evaluation of chemotherapy efficacy but also for patient suitability prediction of chemotherapy outcomes, although a larger and wider range of sample cohorts was required. It could be concluded that serum metabolites were sensitively responsive to TPF induction chemotherapy and that the metabolites related to glycolysis, redox balance, and anabolic activity were beneficial to the evaluation and prediction of induction chemotherapy outcomes, illustrating the potentials of personalized induction chemotherapy in OSCC patients.

ASSOCIATED CONTENT

Supporting Information

Table S1. Metabolites identified in QC sample. Table S2. Pairwise Pearson correlation coefficients among QC replicates throughout the serum metabolomic investigation. Table S3. Alterations of the differential metabolites among the samples. Table S4. Pathways and metabolites related to induction chemotherapy effects. Figure S1. Analytical procedures in pseudotargeted mode. Figure S2. Flowchart of potential biomarker discovery and the performance evaluation with respect to induction chemotherapy efficacy. Figure S3. Flowchart of potential biomarker discovery and the performance evaluation with respect to patient suitability for induction chemotherapy. Figure S4. Fold changes of S/N of the metabolites acquired in the SIM mode compared with those obtained in full scan mode. Figure S5. EIC and SIM projections of 12 typical trimethylsilyl (TMS) derivatives. Figure S6. Analytical performances of the pseudotargeted metabolomics. Figure S7. PLS-DA model of the samples. Figure S8. Heat map of the correlations among the differential metabolites. Figures S9 and S10. Changes in metabolites in response to induction chemotherapy. Figures S11−S18. Box plots of metabolites significantly associated with chemotherapy efficacy. Figure S19. PCA score plot of NSPre and SPre samples based on the information of 13 differential metabolites. Figure S20. Diagnostic performances of key metabolites related to chemotherapy efficacy. Figure S21. Metabolic alterations in differential metabolites according to tumor size. This material is available free of charge via the Internet at http://pubs.acs.org.

AUTHOR INFORMATION

Corresponding Authors

*Laiping Zhong: Tel: +86-21-23271699-5160. Fax: +86-21-63136856. E-mail: zhonglp@hotmail.com.

*Guowang Xu: Tel/Fax: 0086-411-84379559. E-mail: xugw@dicp.ac.cn.

Author Contributions

§G.Y. and Y.L. contributed equally to this work.

Notes

The authors declare no competing financial interest.

ACKNOWLEDGMENTS

The study has been supported by the foundations (No. 21175132, No. 21375127) and the creative research group project (No. 21321064) from the National Natural Science Foundation of China.

ABBREVIATIONS

OSCC, oral squamous cell carcinoma; TPF, docetaxel, cisplation and fluorouracil; GC−MS, gas chromatography−mass spectrometry; MSTFA, *N*-methyl-*N*-(trimethylsilyl)-trifluoroacetamide; SPre, prechemotherapy patients whose chemotherapy efficacy was significant; SPost, postchemotherapy patients whose efficacy were significant; NSPre, prechemotherapy patients whose efficacy were not significant; NSPost, postchemotherapy patients whose efficacy was not significant; S, patients whose efficacy was significant; NS, patients whose efficacy was not significant; QC, quality control; SIM, selected ion monitoring; S/N, signal-to-noise; PCA, principal component analysis; PLS-DA, partial least-squares discriminant analysis; VIP, variable importance in the projection; RF, random forest; MCCV, Monte Carlo cross validation; ROC, receiver operating characteristic; AUC, area under the curve

REFERENCES

(1) Neville, B. W.; Day, T. A. Oral cancer and precancerous lesions. *Ca-Cancer J. Clin.* **2002**, *52* (4), 195−215.

(2) Parkin, D. M.; Bray, F.; Ferlay, J.; Pisani, P. Global cancer statistics, 2002. *Ca-Cancer J. Clin.* **2005**, *55* (2), 74−108.

(3) Pignon, J.-P.; le Maitre, A.; Maillard, E.; Bourhis, J.; Grp, M.-N. C. Meta-analysis of chemotherapy in head and neck cancer (MACH-NC): An update on 93 randomised trials and 17,346 patients. *Radiother. Oncol.* **2009**, *92* (1), 4−14.

(4) Zhong, L. P.; Zhang, C. P.; Ren, G. X.; Guo, W.; William, W. N., Jr.; Sun, J.; Zhu, H. G.; Tu, W. Y.; Li, J.; Cai, Y. L.; Wang, L. Z.; Fan, X. D.; Wang, Z. H.; Hu, Y. J.; Ji, T.; Yang, W. J.; Ye, W. M.; He, Y.; Wang, Y. A.; Xu, L. Q.; Wang, B. S.; Kies, M. S.; Lee, J. J.; Myers, J. N.; Zhang, Z. Y. Randomized phase III trial of induction chemotherapy with docetaxel, cisplatin, and fluorouracil followed by surgery versus up-front surgery in locally advanced resectable oral squamous cell carcinoma. *J. Clin. Oncol.* **2013**, *31* (6), 744−751.

(5) Pignon, J.; Bourhis, J.; Domenge, C.; Designe, L. Chemotherapy added to locoregional treatment for head and neck squamous-cell carcinoma: three meta-analyses of updated individual data. *Lancet* **2000**, *355* (9208), 949−955.

(6) Tan, Y.; Yin, P.; Tang, L.; Xing, W.; Huang, Q.; Cao, D.; Zhao, X.; Wang, W.; Lu, X.; Xu, Z.; Wang, H.; Xu, G. Metabolomics study of stepwise hepatocarcinogenesis from the model rats to patients: potential biomarkers effective for small hepatocellular carcinoma diagnosis. *Mol. Cell. Proteomics* **2012**, *11* (2), M111.010694.

(7) Chen, J.; Zhang, X.; Cao, R.; Lu, X.; Zhao, S.; Fekete, A.; Huang, Q.; Schmitt-Kopplin, P.; Wang, Y.; Xu, Z.; Wan, X.; Wu, X.; Zhao, N.;

Xu, C.; Xu, G. Serum 27-nor-5beta-cholestane-3,7,12,24,25 pentol glucuronide discovered by metabolomics as potential diagnostic biomarker for epithelium ovarian cancer. *J. Proteome Res.* **2011**, *10* (5), 2625−2632.
(8) Wei, S.; Liu, L.; Zhang, J.; Bowers, J.; Gowda, G. A.; Seeger, H.; Fehm, T.; Neubauer, H. J.; Vogel, U.; Clare, S. E.; Raftery, D. Metabolomics approach for predicting response to neoadjuvant chemotherapy for breast cancer. *Mol. Oncol.* **2013**, *7* (3), 297−307.
(9) Roodhart, J. M. L.; Daenen, L. G. M.; Stigter, E. C. A.; Prins, H.-J.; Gerrits, J.; Houthuijzen, J. M.; Gerritsen, M. G.; Schipper, H. S.; Backer, M. J. G.; van Amersfoort, M.; Vermaat, J. S. P.; Moerer, P.; Ishihara, K.; Kalkhoven, E.; Beijnen, J. H.; Derksen, P. W. B.; Medema, R. H.; Martens, A. C.; Brenkman, A. B.; Voest, E. E. Mesenchymal Stem Cells Induce Resistance to Chemotherapy through the Release of Platinum-Induced Fatty Acids. *Cancer Cell* **2011**, *20* (3), 370−383.
(10) Weaver, Z.; Difilippantonio, S.; Carretero, J.; Martin, P. L.; El Meskini, R.; Iacovelli, A. J.; Gumprecht, M.; Kulaga, A.; Guerin, T.; Schlomer, J.; Baran, M.; Kozlov, S.; McCann, T.; Mena, S.; Al-Shahrour, F.; Alexander, D.; Wong, K. K.; Van Dyke, T. Temporal Molecular and Biological Assessment of an Erlotinib-Resistant Lung Adenocarcinoma Model Reveals Markers of Tumor Progression and Treatment Response. *Cancer Res.* **2012**, *72* (22), 5921−5933.
(11) Backshall, A.; Sharma, R.; Clarke, S. J.; Keun, H. C. Pharmacometabonomic profiling as a predictor of toxicity in patients with inoperable colorectal cancer treated with capecitabine. *Clin. Cancer Res.* **2011**, *17* (9), 3019−3028.
(12) Ye, G.; Zhu, B.; Yao, Z.; Yin, P.; Lu, X.; Kong, H.; Fan, F.; Jiao, B.; Xu, G. Analysis of urinary metabolic signatures of early hepatocellular carcinoma recurrence after surgical removal using gas chromatography−mass spectrometry. *J Proteome Res* **2012**, *11* (8), 4361−4372.
(13) Li, Y.; Ruan, Q.; Li, Y.; Ye, G.; Lu, X.; Lin, X.; Xu, G. A novel approach to transforming a non-targeted metabolic profiling method to a pseudo-targeted method using the retention time locking gas chromatography/mass spectrometry-selected ions monitoring. *J. Chromatogr., A* **2012**, *1255*, 228−236.
(14) Chen, S.; Kong, H.; Lu, X.; Li, Y.; Yin, P.; Zeng, Z.; Xu, G. Pseudotargeted Metabolomics method and its application in serum biomarker discovery for hepatocellular carcinoma based on ultra gigh-performance liquid chromatography/triple quadrupole mass spectrometry. *Anal. Chem.* **2013**, *85* (17), 8326−8333.
(15) Licitra, L.; Grandi, C.; Guzzo, M.; Mariani, L.; Lo Vullo, S.; Valvo, F.; Quattrone, P.; Valagussa, P.; Bonadonna, G.; Molinari, R.; Cantu, G. Primary chemotherapy in resectable oral cavity squamous cell cancer: A randomized controlled trial. *J. Clin. Oncol.* **2003**, *21* (2), 327−333.
(16) Saeed, A. I.; Bhagabati, N. K.; Braisted, J. C.; Liang, W.; Sharov, V.; Howe, E. A.; Li, J.; Thiagarajan, M.; White, J. A.; Quackenbush, J. TM4 microarray software suite. *Methods Enzymol.* **2006**, *411*, 134−193.
(17) Xia, J.; Mandal, R.; Sinelnikov, I. V.; Broadhurst, D.; Wishart, D. S. MetaboAnalyst 2.0–a comprehensive server for metabolomic data analysis. *Nucleic Acids Res.* **2012**, *40* (W1), W127−W133.
(18) Chong, I.-G.; Jun, C.-H. Performance of some variable selection methods when multicollinearity is present. *Chemom. Intell. Lab. Syst.* **2005**, *78* (1), 103−112.
(19) Wold, S.; Sjöström, M.; Eriksson, L. PLS-regression: a basic tool of chemometrics. *Chemom. Intell. Lab. Syst.* **2001**, *58* (2), 109−130.
(20) Breiman, L. Random forests. *Mach. Learn.* **2001**, *45* (1), 5−32.
(21) Ronchetti, E.; Field, C.; Blanchard, W. Robust linear model selection by cross-validation. *J. Am. Stat. Assoc.* **1997**, *92* (439), 1017−1023.
(22) Shao, J. Linear model selection by cross-validation. *J. Am. Stat. Assoc.* **1993**, *88* (422), 486−494.
(23) Xu, Q.-S.; Liang, Y.-Z. Monte Carlo cross validation. *Chemom. Intell. Lab. Syst.* **2001**, *56* (1), 1−11.
(24) Gika, H. G.; Theodoridis, G. A.; Wingate, J. E.; Wilson, I. D. Within-day reproducibility of an HPLC-MS-Based method for metabonomic analysis: application to human urine. *J. Proteome Res.* **2007**, *6* (8), 3291−3303.
(25) Begley, P.; Francis-McIntyre, S.; Dunn, W. B.; Broadhurst, D. I.; Halsall, A.; Tseng, A.; Knowles, J.; Goodacre, R.; Kell, D. B. Consortium, H., Development and Performance of a Gas Chromatography-Time-of-Flight Mass Spectrometry Analysis for Large-Scale Nontargeted Metabolomic Studies of Human Serum. *Anal. Chem.* **2009**, *81* (16), 7038−7046.
(26) *Guidance for Industry: Bioanalytical Method Validation*; U.S. Department of Health and Human Services, Food and Drug Administration, Center for Drug Evaluation and Research (CDER), Center for Veterinary Medicine (CVM), May 2001. http://www.fda.gov/downloads/drugs/guidancecomplianceregulatoryinformation/guidances/ucm070107.pdf.
(27) Keun, H. C.; Sidhu, J.; Pchejetski, D.; Lewis, J. S.; Marconell, H.; Patterson, M.; Bloom, S. R.; Amber, V.; Coombes, R. C.; Stebbing, J. Serum Molecular Signatures of Weight Change during Early Breast Cancer Chemotherapy. *Clin. Cancer Res.* **2009**, *15* (21), 6716−6723.
(28) Wang, J.; Alexander, P.; Wu, L.; Hammer, R.; Cleaver, O.; McKnight, S. L. Dependence of mouse embryonic stem cells on threonine catabolism. *Science* **2009**, *325* (5939), 435−439.
(29) Shyh-Chang, N.; Locasale, J. W.; Lyssiotis, C. A.; Zheng, Y.; Teo, R. Y.; Ratanasirintrawoot, S.; Zhang, J.; Onder, T.; Unternaehrer, J. J.; Zhu, H.; Asara, J. M.; Daley, G. Q.; Cantley, L. C. Influence of Threonine Metabolism on S-Adenosylmethionine and Histone Methylation. *Science* **2013**, *339* (6116), 222−226.
(30) Balendiran, G. K.; Dabur, R.; Fraser, D. The role of glutathione in cancer. *Cell Biochem. Funct.* **2004**, *22* (6), 343−352.
(31) Kaddurah-Daouk, R.; Weinshilboum, R. M. Pharmacometabolomics: implications for clinical pharmacology and systems pharmacology. *Clin. Pharmacol. Ther.* **2014**, *95* (2), 154−167.
(32) Clayton, T. A.; Lindon, J. C.; Cloarec, O.; Antti, H.; Charuel, C.; Hanton, G.; Provost, J. P.; Le Net, J. L.; Baker, D.; Walley, R. J.; Everett, J. R.; Nicholson, J. K. Pharmaco-metabonomic phenotyping and personalized drug treatment. *Nature* **2006**, *440* (7087), 1073−1077.